Eduction of Unsteady Structure in a Turbulent Jet by Use of Continuous and Discrete Wavelet Transforms*[1]

By Hui Li,*[2] Masahiro Takei,*[3] Mitsuaki Ochi,*[3]
Yoshifuru Saito*[4] and Kiyoshi Horii*[5]

Key Words: Continuous Wavelet Transform, Discrete Wavelet Transform, Eddy, Jet, Multiresolution Analysis, Turbulence, Unsteady Structure

Abstract

To evaluate unsteady eddy structures of a plane turbulent jet in the dimension of time and scale, velocity signals were analyzed using continuous and discrete wavelet transforms in this paper. By analyzing the distribution of coefficients of continuous wavelet transform, localized nearly periodic eddy motions with $a=64$, 100 and 180 ms were observed in the shear layer of $x/d=8.5$ in the time ranges of $t=0$–220, 280–600 and 680–1000 ms, respectively. From multiresolution analysis or discrete wavelet transform, the peak that appears in the component of fluctuating velocity represented the passing of eddy through the shear layer and concentration of the energy of the flow at one instant. The intermittent eddy phenomenon or zero components of fluctuating velocity can be observed at higher levels or smaller scales.

1. Introduction

The large-scale eddy motion in a plane turbulent jet exhibits a symmetric, periodic and apparent flapping motion in the similar region, and the evolution and interaction of large-scale organized structures play an important role in spreading turbulent jet and momentum transfer. Until now, conventional statistical methods such as space-time correlation functions, spectra, coherent functions, conditional sampling methods and visualization techniques, were well-established usual techniques for gaining information regarding the nature of turbulent structures or eddy motion. However, turbulence or eddy motion is characterized by unsteady and localized structures of multiple spatial scales. Some important spatial information is lost owing to the non-local nature of the Fourier analysis. The visualization of organized motion in shear layers also showed that conditional sampling measurement had been hiding very important features of turbulence.

Within the last decade, there has been growing interest in the wavelet analysis of turbulent signal, which can combine time-space and frequency-space analyses to produce a potentially more revealing picture of time-frequency localization of turbulent structures. The wavelet transform can either be continuous or discrete, and yields elegant decompositions of turbulent flows. The continuous wavelet transform offers a continuous and redundant unfolding in terms of time and scale and can thus track coherent structures.[1-4] Besides these application studies, several new tools and diagnostics based on the wavelet transform, such as wavelet correlation function,[1] wavelet Reynolds stress function,[5] wavelet triple velocity correlation,[5] and local wavelet Reynolds stress function[6] have been developed. They offer the potential to extract new information from various flow fields. The coefficients of continuous wavelet transform can extract the characterization of local regularity continuously, but it is not possible to reconstruct the original function because the mother wavelet function is a non-orthogonal function. In signal processing, it is important to reconstruct the original signal from the wavelet composition and to study multiresolution signals in the range of various scales.

The discrete wavelet transform allows an orthogonal projection on a minimal number of independent modes and is an inevitable, and in fact, orthogonal inverse transform. Such analysis is known as multiresolution representation and might be used to compute or model turbulent flow dynamics. Li et al.[7,8] applied two-dimensional orthogonal wavelets to turbulent images, and extracted multiresolution turbulent structures and a coherent structure. Li et al.[9] also employed the orthogonal vector wavelet transform technique to analyze multi-scale vortical structures in the turbulent near-wake of a circular cylinder. However, few investigations concern the application of discrete wavelet transform to turbulent signals.

*[1] Received September 3rd, 1999.
*[2] Department of Mechanical Engineering, Kagoshima University, Kagoshima, Japan.
*[3] Department of Mechanical Engineering, Nihon University, Tokyo, Japan.
*[4] Department of Electrical & Electronic Engineering, Hosei University, Tokyo, Japan.
*[5] Shirayuri Women's College, Tokyo, Japan.

To evaluate the vortical structures in the dimension of time and scale in a turbulent jet, continuous and discrete wavelet transforms were applied to the velocity signals of a plane turbulent jet in this paper.

2. Continuous Wavelet Transform

For any signal, $f(t)\in L^p(\mathscr{R})$ $1\le p\le\infty$ ($L^p(\mathscr{R})$ denotes the Hilbert space of measure) the continuous wavelet transform can be defined as:

$$Wf(b,a)=\frac{1}{a}\int_{-\infty}^{\infty} f(t)\bar{\psi}\left(\frac{t-b}{a}\right)dt, \qquad \ldots.(1)$$

where $Wf(b,a)$ is called the wavelet coefficient, a is the wavelet scale or dilation, and b is the analyzing position. $\psi(t)$ is a function of $L^2(\mathscr{R})$ called an analyzing wavelet or mother wavelet (here $\bar{}$ stands for complex conjugate).

It is well-known that several functions, such as Haar, Paul, French hat, m-th derivatives of the Gaussian, Mexican hat, Morlet and Gabor functions, are commonly used as analyzing wavelets. The choice of the appropriate wavelet function is of the flexibility and depends on the kind of information that we want to extract from the signal. In this paper, we employ the Morlet wavelet, a complex-valued function, to analyze our problems. It is defined as:

$$\psi(t)=e^{-i\omega_0 t}e^{-t^2/2} \quad \text{and} \quad \hat{\psi}(\omega)=\sqrt{2\pi}e^{-(\omega-\omega_0)^2/2}. \qquad \ldots.(2)$$

It is obvious that the Morlet wavelet is localized around $t=0$, and $\hat{\psi}(\omega)$ is localized around the central frequency $\omega_c=\omega_0$. In practical applications of signal processing, it has been found that a particularly useful value for the central frequency ω_c is the one for which wavelet scale a presents the period or frequency. Li[1] defined the central frequency as $\omega_c=\omega_0=2\pi$. Hence, $(1/a)\bar{\psi}((t-b)/a)$ is localized around position b and central frequency $2\pi/a$; i.e., wavelet scale a becomes a period parameter. Therefore, the wavelet coefficient of Eq. (1) can describe a signal as localized strength of the signal over a time-period plane.

3. Discrete Wavelet Transform

In this section, we introduce the definition of discrete wavelet transform from the view of a matrix.

The discrete wavelet transform is a transformation of information from a fine scale to a coarser scale by extracting information that describes the fine scale variability (the detail coefficients or wavelet coefficients) and the coarser scale smoothness (the smooth coefficients or mother-function coefficients) according to:

$$\{S_j\}=[H]\{S_{j+1}\} \quad \text{and} \quad \{D_j\}=[G]\{S_{j+1}\}, \qquad \ldots.(3)$$

where $\boldsymbol{S}$ represents mother-function coefficients, $\boldsymbol{D}$ represents wavelet coefficients, j is the wavelet level, and $\boldsymbol{H}$ and $\boldsymbol{G}$ are the convolution matrices based on the wavelet basis function. High values of j signify finer scales of information. The complete wavelet transform is a process that recursively applied Eq. (3) from the finest to the coarsest wavelet level (scale). This describes a scale-by-scale extraction of the variability information at each scale. The mother-function coefficients generated at each scale are used for extraction in the next coarser scale.

The inverse discrete wavelet transform is similarly implemented via a recursive recombination of the smooth and detailed information from the coarsest to finest wavelet level (scale):

$$\{S_{j+1}\}=[H]^{\mathrm{T}}\{S_j\}+[G]^{\mathrm{T}}\{D_j\}, \qquad \ldots.(4)$$

where $\boldsymbol{H}^{\mathrm{T}}$ and $\boldsymbol{G}^{\mathrm{T}}$ indicate the transpose of $\boldsymbol{H}$ and $\boldsymbol{G}$ matrices, respectively.

Matrices $\boldsymbol{H}$ and $\boldsymbol{G}$ are created from the coefficients of basis functions, and represent the convolution of basis functions with the data.

Many different orthonormal wavelet basis functions, such as Harr basis, Daubechies basis, Meyer basis, Spline basis and Coiflets basis, were often used in the discrete wavelet transform. Different wavelet basis functions will preferentially move, between scales, different characteristics of the target data sets. For example, use of the Harr basis function may emphasize discontinuity in the target data sets, and the Daubechies family may emphasize the smoothness of the analyzed data. In this paper, we use the Daubechies member with order 20 as the wavelet basis function, which has either smoothness in physical space or most localization in frequency space. For illustration, the simplest (and most localized) Daubechies member with order 4, having only four coefficients, c_0, c_1, c_2 and c_3, is given by the following matrix:

$$\begin{bmatrix}
c_0 & c_1 & c_2 & c_3 & & & & & & & & \\
c_3 & -c_2 & c_1 & -c_0 & & & & & & & & \\
 & & c_0 & c_1 & c_2 & c_3 & & & & & & \\
 & & c_3 & -c_2 & c_1 & -c_0 & & & & & & \\
 & & & & & & \ddots & & & & & \\
 & & & & & & & & & & & \\
 & & & & & & & & & & & \\
 & & & & & & & & c_0 & c_1 & c_2 & c_3 \\
 & & & & & & & & c_3 & -c_2 & c_1 & -c_0 \\
c_2 & c_3 & & & & & & & & & c_0 & c_1 \\
c_1 & -c_0 & & & & & & & & & c_3 & -c_2
\end{bmatrix}, \qquad \ldots.(5)$$

where blank entries signify zero. The action of the matrix, overall, is thus to perform two related convolutions, then to decimate each of them by half and interleave the remaining halves. It is useful to think of the coefficients c_0, c_1, c_2 and c_3 as a smoothing filter called matrix $\boldsymbol{H}$, something like a moving average of four points. Then,

because of the minus signs, coefficient, c_3, $-c_2$, c_1 and $-c_0$, call it matrix $\boldsymbol{G}$, are not a smoothing filter.

4. Experimental Apparatus

A definition sketch of the plane jet is shown in Fig. 1, where x is the streamwise coordinate, and y is the lateral coordinate. The jet is generated by a blower-type wind tunnel having flow-straightening elements, screens, and settling length, and a 24:1 contraction leading to a 350×25 mm nozzle (the nozzle width d is 25 mm). For all measurements, the jet is operated at a constant Reynolds number $Re = 3330$ (exit velocity is 2 m/s) based upon nozzle width d. The velocity of x-component of the jet is measured simultaneously using a standard hot-wire anemometer located in the (x, y)-plane. The recording frequency is 2 kHz. The measurements presented in this paper were taken on the centerline and in the shear layer.

5. Results and Discussion

5.1. Visualization of eddy motion Figure 2 shows images of the plane turbulent jet in our experiment, which were obtained by a high-speed video camera. The vortex street structures are clearly observed, and the large-scale eddy motions are unsteady and localized structures. The scale of the eddy is always changing with respect to time at any position.

5.2. Identification of unsteady eddy motion utilizing the continuous wavelet transform In general, structure features were inferred from the statistics analysis of measurements, and the analysis of unsteady structures was made from visual observations. Yule[10] presented experimental evidence to show that when an eddy current moves close to the centerline, the local fluctuating velocity appears as unusually large positive and negative peaks. However, from these peaks of velocity signals, local or unsteady information at different scales (i.e., the localized eddy structure of multiple scale) is unable to be determined. To identify the local characteristics of flow structure in a plane jet, we analyze the fluctuating velocity, which was measured on the centerline at $x/d = 8.5$, by continuous wavelet transform. Figure 3 shows the decomposition of the fluctuating velocity in both period and time spaces with the help of the Morlet wavelet. The unsteady flow structure is represented using the real part $Wf(t, a)$ and phase $\theta Wf(t, a)$ of the wavelet coefficient (abscissa: time t, ordinate: period a, black & white for magnitudes of wavelet coefficients), and the velocity fluctuation is also plotted at the bottom of the figures. Figure 3 displays that every positive or negative peak in the large-period region consists of positive and negative peaks in the smaller period region, and gives us a map of the successive branching structure. For example, a peak at $a = 190$ ms around $t = 470$ ms consists of negative and positive peaks at $a = 100$ ms. This means a large eddy contains two smaller eddies at this time t. In Fig. 3, it is also evident that the strong periodic peaks appear around $a = 64$, 100 and 180 ms in the ranges of $t = 0$–220, 280–600 and 680–1000 ms, respectively. These peaks imply the passing of eddy through the shear layer. The periods of peaks (i.e. scales of eddy) increase with time. This indicates that although the local scale of motion always changes, localized nearly periodic eddy motions exist in unsteady turbulent jet. Making a comparison between $Wf(t, a)$ and fluctuating velocity, we found that the successive negative and positive peaks in fluctuating velocity from $t = 110$–140 ms correspond to successive negative and positive peaks of $Wf(t, a)$ around $a = 64$ ms. This implies the passing of nearly periodic eddy with $a = 64$ ms through the shear layer at this time interval. The same phenomenon may also be observed in the ranges of $t = 280$–600 ms and $t = 680$–1000 ms. From the distribution of $Wf(t, a)$ it can be observed that two stronger positive peaks with $a = 100$

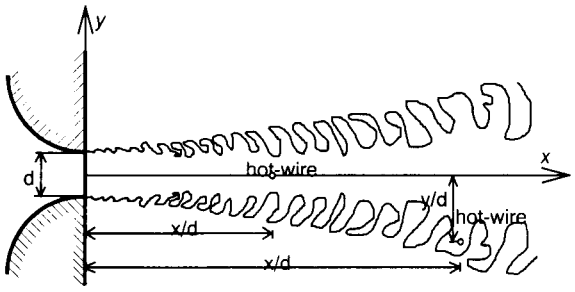

Fig. 1. Sketch of the experimental configuration.

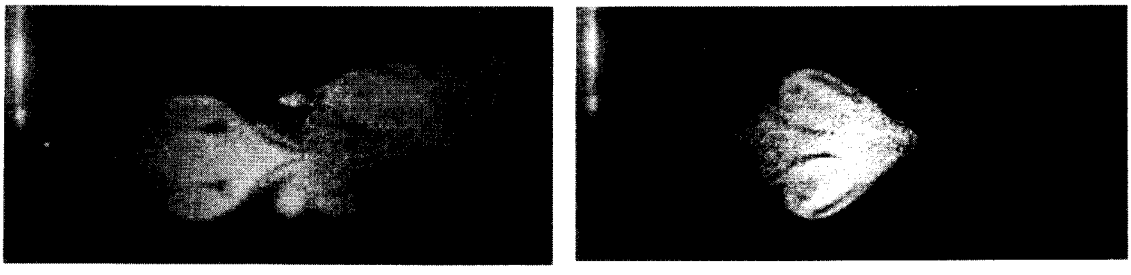

(a) $t = 0$ ms (b) $t = 24$ ms

Fig. 2. Flow images of a plane jet.

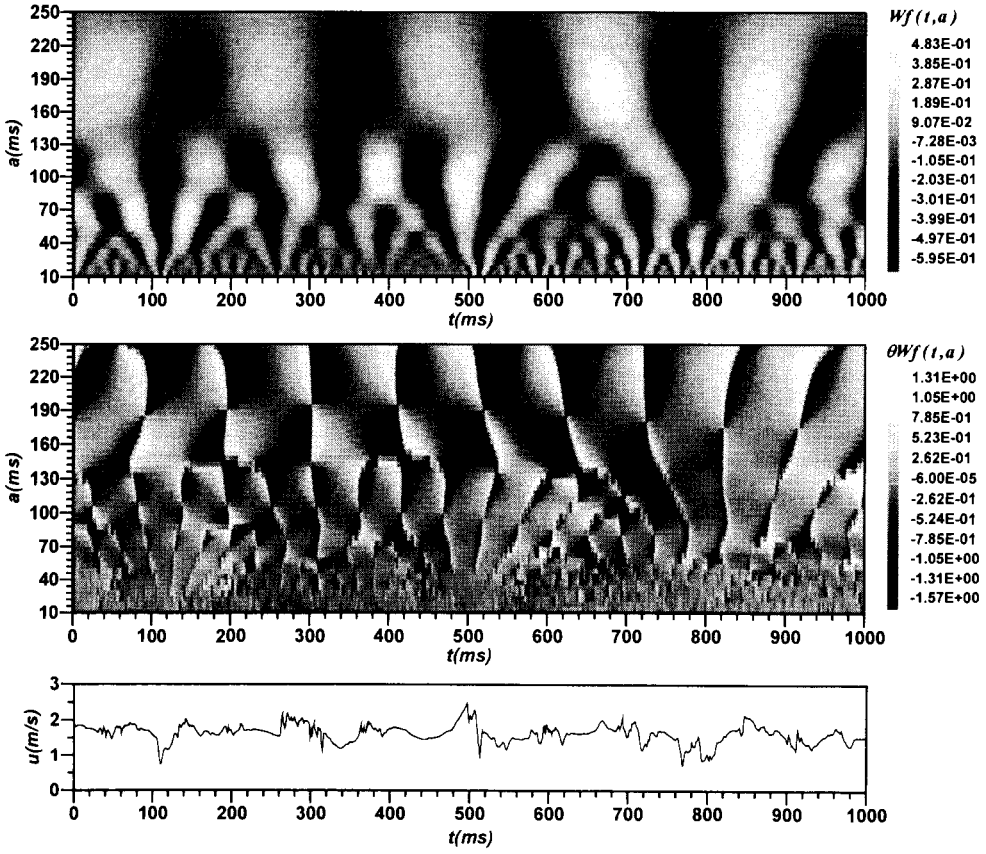

Fig. 3. Continuous wavelet transform of fluctuating velocity on the centerline at $x/d=8.5$.

and 180 ms appear in the neighborhood of $t=850$ ms. These two peaks correspond to two peaks within a small peak at $t=850$ ms and a larger peak within the range of $t=800$–900 ms, respectively. This structure in $Wf(t, a)$ indicates that two eddies with $a=100$ ms and 180 ms pass through the shear layer at this instant, and a larger-scale eddy contains a smaller-scale eddy.

It is well-known that $\theta Wf(t, a)$ expresses the phase of wavelet coefficient or the phase of a signal at various periods, and is employed to search the irregular part of signals. From the definition of $\theta Wf(t, a)$, the discontinuous constant phase lines correspond to the zero lines of $Wf(t, a)$. It is found that the region of the positive or negative peak in $Wf(t, a)$ is equivalent to the range of zero $\theta Wf(t, a)$. It is obvious that $\theta Wf(t, a)$ exhibits the regular pattern for scale $a>140$ ms. This indicates the periodic large-scale eddy motions, which can also be observed from the distribution of alternative peaks in $Wf(t, a)$ around $a=180$ ms.

From the above analysis, we can say that an important purpose for using continuous wavelet transform is to extract peak distributions from the wavelet coefficient because they correspond to the maximum or minimum strength of velocity fluctuation at various periods and represent the eddy motions with various scales.

5.3. Analysis of unsteady eddy motion utilizing the discrete wavelet transform Differing from the continuous wavelet transform, the inverse discrete wavelet transform can be easily carried out due to the existence of the orthonormal wavelet basis functions. In this paper, we first compute the wavelet coefficients of fluctuating velocity using Eq. (3) with the help of the Daubechies wavelet of order 20. Then the inverse discrete wavelet transform is applied to wavelet coefficients at each wavelet level, and components of fluctuating velocity are obtained at each level or scale. This procedure is called multiresolution analysis or orthogonal decomposition of the signal. The components of fluctuating velocity on the centerline at $x/d=8.5$ ranged from wavelet level 1 to 7, which correspond to the scale range $a=200$–1 ms, and are shown in Fig. 4. This figure represents the time behavior of the fluctuating velocity within different scale bands, and gives their contribution to the total energy. It is apparent that large peaks distribute in the range of level 1 to 3, which correspond to scale $a=200$–65 ms approximately. These peaks imply the passing of dominant eddies through the shear layer. This scale range is dynamically quite important and concentrates much of the energy of the flow. The apparent peaks appear at every level around $t=0.5$ s, which corresponds to the large peaks in the original fluctuating velocity. This indicates that a large-scale eddy containing eddies of various scale is passing the shear layer of this position at these two instances, because the time interval of a large positive peak at level 1 contains several positive and negative peaks at other levels or smaller scales. This

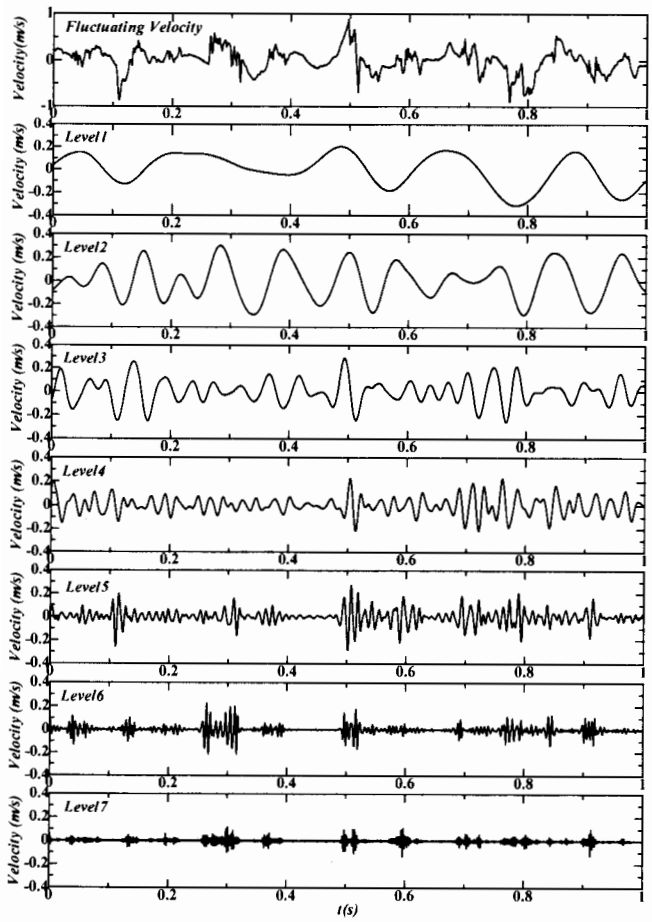

Fig. 4. Multiresolution decomposition of fluctuating velocity on the centerline at $x/d=8.5$ based on discrete wavelet transform.

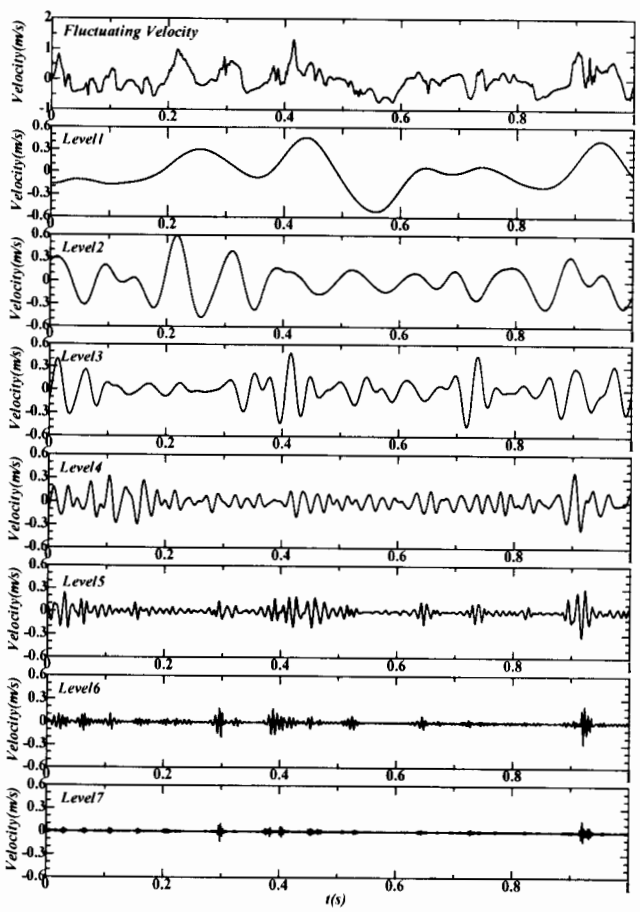

Fig. 5. Multiresolution decomposition of fluctuating velocity in the shear layer of $x/d=5$ and $y/d=0.4$ based on discrete wavelet transform.

flow structure contains the large energy at this moment, and the flow image may be inferred as Fig. 2(b). At a higher level (level 6 and 7) or smaller scale, the zero fluctuating velocity appears in some time range, for example $t=0.4$–0.48 s, which is similar to the intermittent phenomenon. This indicates that the flow structures don't exist in the passing eddy at this scale band and time interval, and only have mean or convective velocity. This phenomenon may be called the intermittent eddy.

Figure 5 plots the components of fluctuating velocity with wavelet levels 1–7 in the shear layer of $x/d=5$ and $y/d=0.4$, which also correspond to the scale range $a=200$–1 ms. It can be observed that the largest positive peak appears at level 2 around time $t=2.2$ s, which corresponds to the large positive peaks in the original fluctuating velocity, and the peaks at other levels are smaller. This phenomenon indicates that this level or scale band concentrates much of the energy of the turbulent flow at this instant. Although a large positive peak appears at level 1 in the range of $t=0.85$–1 s, large peaks can also be observed at other levels. This means that the energy of the turbulent flow distributes among various scales and smaller eddies exist in a large eddy.

6. Summary

In this paper, the vortical structures of a plane turbulent jet were evaluated in the dimensions of time and scale using continuous and discrete wavelet transforms. The following results can be summarized.

(1) The distribution of coefficients of continuous wavelet transform indicates that localized nearly periodic eddy motions with $a=64$, 100 and 180 ms appear in the shear layer of x $d=8.5$ in the time ranges of $t=0$–220, 280–600 and 680–1000 ms, respectively.

(2) From multiresolution analysis, the peak of fluctuating velocity component represents the passing of eddies through the shear layer and concentration of the energy of the flow at one instant.

(3) At a higher level or smaller scale, the zero components of fluctuating velocity appear in some time ranges, which are called intermittent eddy phenomenon.

(4) A large peak appears at some level and components of fluctuating velocity at other levels are smaller at some time. This phenomenon indicates that this level or scale band concentrates much of the energy of the turbulent flow at this instant.

References

1) Li, H.: Identification of Coherent Structure in Turbulent Shear Flow with Wavelet Correlation Analysis, *Trans. ASME, J. Fluids Eng.*, **120**, 4 (1998), pp. 778–785.
2) Li, H.: Wavelet Auto-Correlation Analysis Applied to Eddy Structure Identification of Free Turbulent Shear Flow, *JSME Int. J. Fluids Therm. Eng.*, **40**, 4 (1997), pp. 567–576.
3) Li, H. and Nozaki, T.: Application of Wavelet Cross-Correlation Analysis to a Plane Jet, *JSME Int. J. Fluids Therm. Eng.*, **40**, 1 (1997), pp. 58–66.
4) Li, H. and Nozaki, T.: Wavelet Analysis for the Plane Turbulent Jet (Analysis of Large Eddy Structure), *JSME Int. J. Fluids Therm. Eng.*, **38**, 4 (1995), pp. 525–531.
5) Li, H.: Wavelet Statistical Analysis of the near Field Flow Structure in a Turbulent Jet. *Trans. Japan Soc. Aero. Space Sci.*, **41**, 133 (1998), pp. 132–139.
6) Li, H., Nozaki, T., Tabata, T. and Oshige, S.: Wavelet Analysis of the Near-Field Structure in a Bounded Jet, *Trans. Japan Soc. Aero. Space Sci.*, **42**, 135 (1999), pp. 27–33.
7) Li, H., Takei, M., Ochi, M., Saito, Y. and Horii, K.: Application of Two-dimensional Orthogonal Wavelets to Multiresolution Image Analysis of a Turbulent Jet, *Trans. Japan Soc. Aero. Space Sci.*, **42**, 137 (1999), pp. 120–127.
8) Li, H., Takei, M., Ochi, M., Saito, Y. and Horii, K.: Effect of Different Orthogonal Wavelet Basis on Multiresolution Image Analysis of a Turbulent Flow, *Proceedings of The International Conference on Optical Technology and Image Processing in Fluid, Thermal and Combustion Flow*, No. AB015 (1998), pp. 1–11.
9) Li, H., Zhou, Y., Takei, M., Ochi, M., Saito, Y. and Horii, K.: Visualization of Multi-Scale Turbulent Structures Using Orthogonal Wavelet Transform, *Album of Visualization*, **16** (1999), pp. 11–12.
10) Yule, A. J.: Large-scale Structure in the Mixing Layer of a Round Jet, *J. Fluid Mech.*, **89** (1978), pp. 413–432.